Structural Transformations of Ice at Normal and High Pressures via Molecular Dynamics Simulations

Tamotsu Hashimoto,* Shin Sugawara, and Yasuaki Hiwatari

Physics Department, Faculty of Science, Kanazawa University, Kanazawa, 920-11 Japan

Received: October 15, 1996; In Final Form: June 17, 1997[⊗]

Molecular dynamics simulation was carried out to investigate structural phase transitions of ice in high-pressure phases. Transition from ice VIII to ice VII and further to ice X was obtained on applying pressure. Transition from ice VIII to ice VII on heating was also successfully reproduced. Ice VII thus obtained was orientationally disordered, while ice VII in high pressure was highly ionized, which is in good agreement with experiments. Another series of MD simulations were done to investigate high-pressure and high-temperature forms of ice. First, on heating, transition from amorphous ice to ice X was obtained, which is an order−disorder transition with respect to the oxygens. Then, on further heating, ice X was transformed into another form of ice in which the oxygen lattice forms an fcc structure and protons are almost in a gas state. Although the KKY potential that we have used in the present MD simulation is the one originally developed for low-pressure ice and water, it turns out that it can be applicable to the high-pressure phases of ice with predictions in agreement with experiments.

1. Introduction

Ice has more than 10 different stable phases.[1] In the low-pressure regime, the structure of ice is complex, while in the high-pressure regime over 2 GPa, it becomes simpler. At a pressure above 2 GPa and temperature above 270 K, ice VII appears, in which oxygens form a bcc lattice and hydrogens are disordered. At a pressure above 2 GPa and a temperature below 270 K, ice VIII appears, in which oxygens form a bcc-like lattice and hydrogens are in an ordered state. Above 80 GPa, hydrogen-bond-symmetrized ice, called ice X, in which the oxygen lattice is also bcc, is supposed to appear.[2,3] Because of such simplicity of structures of ice in such a high-pressure regime, it is easy to perform molecular dynamics (MD) simulations and to study phase transformations.

Ice X is characterized by the structure in which the oxygens form a bcc lattice and hydrogens are located at the midpoint of two nearest oxygens; namely, hydrogen bonds are symmetrized.[2−9] Several experiments have been done on ice X. Polian *et al.* have reported that by compression of ice VII at 300 K up to 67 GPa the VII−X transition occurs at 44 GPa.[6] Hemley *et al.* have reported that up to 128 GPa at room temperature, the bcc lattice of oxygens continues to exist.[7] Pruzan *et al.* studied the VII−VIII phase boundary up to about 70 GPa and suggested that the ice X might appear only above 80 Gpa.[2,3] Recently Goncharov *et al.* showed that it appeared at 60 GPa.[10]

In MD simulations, rigid molecular models are often used as models of water or ice. However, they are useless for the present work, since at high pressures, water molecules are possibly changed in their molecular structures from those of water molecules at normal pressures. For this reason, in the present work the pair interaction and the three-body interaction between atoms, recently proposed for water and low-pressure ices by Kawamura and co-workers,[11] were used. In this model the system is simply composed of two component atoms (species), hydrogens and oxygens, without any computational condition for forming water molecules. It consists of two-body and three-body interactions as follows:[11]

$$\phi_{2-\mathrm{body}}(r_{ij}) = \frac{z_i z_j}{r_{ij}} + f_0(b_i + b_j)\exp\left(\frac{a_i + a_j - r_{ij}}{b_i + b_j}\right) - \frac{c_i c_j}{r_{ij}^{6}} + f_0 D_{ij}(\exp(-2\beta_{ij}(r_{ij} - r_{ij}^{0})) - 2\exp(-\beta_{ij}(r_{ij} - r_{ij}^{0}))) \quad (1)$$

and

$$\phi_{3-\mathrm{body}}(\theta_{\mathrm{H}_i\mathrm{OH}_j}, r_{\mathrm{OH}_i}, r_{\mathrm{OH}_j}) = -f_k(\cos(2(\theta_{\mathrm{H}_i\mathrm{OH}_j} - \theta_0)) - 1)\sqrt{k(r_{\mathrm{OH}_i})\,k(r_{\mathrm{OH}_j})} \quad (2)$$

where

$$k(r_{\mathrm{OH}_i}) = 1/(\exp(g_r(r_{\mathrm{OH}_i} - r_m)) + 1) \quad (3)$$

In these equations, r_{ij} is an interatomic distance, $\theta_{\mathrm{H}_i\mathrm{OH}_j}$ is an angle between $\mathrm{H}_i-\mathrm{O}-\mathrm{H}_j$ bonds, r_{OH_i} is an $\mathrm{O}-\mathrm{H}_i$ distance, and f_0, z_i, a_i, b_i, c_i, D_{ij}, β_{ij}, r_{ij}^0, f_k, θ_0, g_r, and r_m are parameters that were determined empirically by Kawamura and co-workers so as to reproduce low-pressure ice and water. The two-body interaction (eq 1) consists of Coulomb interactions, short-ranged repulsions, dispersion potentials, and covalent bond potentials which act only between oxygen and hydrogen in each water molecule. On the other hand, the three-body interactions (eq 2) act only for each H−O−H pair. The values of $k(r_{\mathrm{OH}_i})$ and $k(r_{\mathrm{OH}_j})$ (eq 3) define the effective rage of the three-body potential. They are unity in the range of the intramolecular O−H distance and approach zero rapidly over the hydrogen bond distance. The importance of the three-body potentials has been demonstrated by Kawamura and co-workers. Indeed it has been shown that thermal properties of a bulk water and ice I, ice II, and ice IX under normal temperature and pressure were able to be well reproduced with these potentials. The three-body interaction plays an important role in representing a correct angle between H−O−H bonds of water molecules in their bulk systems. Before we carry out the MD simulation on high-pressure ices, it has first been confirmed that such model potentials give a reasonable result for ice VIII at a normal pressure, being consistent with other rigid molecular models.[12−14]

[⊗] Abstract published in *Advance ACS Abstracts,* July 15, 1997.

S1089-5647(96)03160-4 CCC: $14.00

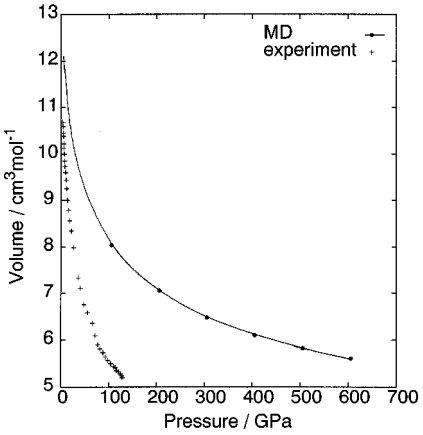

Figure 1. Comparison of the pressure vs the volume of the system obtained by the present model (solid curve) with experimental data (crosses). Dots are the averaged volumes at the corresponding pressures calculated for 4000 time steps. The dots agree with the line, which suggests that the system is nearly relaxed during the pressurization.

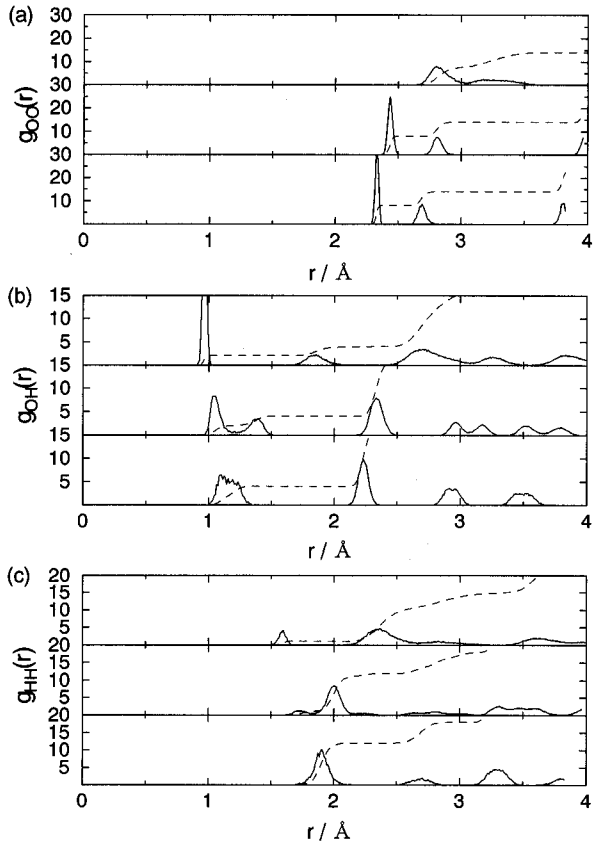

Figure 2. Partial pair distribution functions g_{OO}, g_{OH}, and g_{HH} for simulation I. The dashed curves are the corresponding running coordination number. (a) g_{OO} at 5.7 GPa (ice VIII, upper), 275.7 GPa (ice VII, middle), and 485.7 GPa (ice X, lower). (b and c) g_{OH} and g_{HH}, respectively, with pressures corresponding to those of part a.

In the present MD simulation, in order to realize solid−solid phase transformation, we have used the flexible cell algorithm originally developed by Parrinello and Rahman,[15,16] by means of which the periodically repeating cell can change its shape and volume when the pressure is changed. For example, if the externally applied pressure exceeds a certain value, the system transforms into another lattice structure. To calculate Coulomb interaction, the Ewald method was used.

In the MD experiment I, starting with the initial configuration of ice VIII,[17] we have carried out two runs, simulation I and simulation II. Simulation I is a constant-temperature (100 K) MD calculation,[18] with pressure being increased from 5.7 to 605.7 GPa at the rate of 6 MPa per step (0.2 fs) for 100 000 time steps. Simulation II is a constant-pressure (5.7 GPa) MD calculation, with temperature being increased from 100 to 400 K at the rate of 0.01 K per step for 30 000 time steps, followed by a constant-temperature and constant-pressure MD simulation for 70 000 time steps. In this calculation, the number of particles is chosen to be 192 (64 oxygens and 128 hydrogens), and the time step is taken to be $\Delta t = 0.2$ fs.

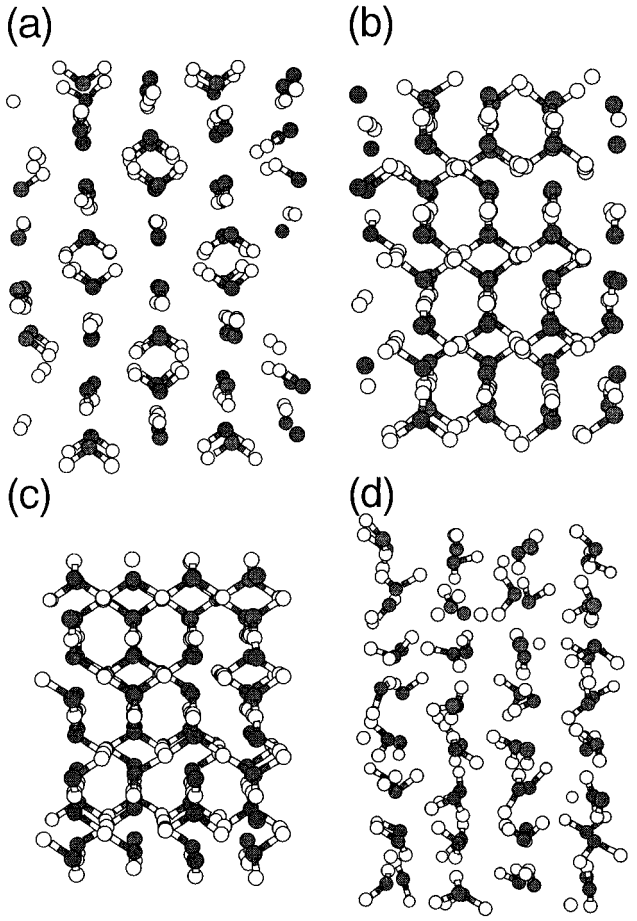

Figure 3. Simulation I (a−c) and simulation II (d). (a) Initial configuration of ice VIII at 5.7 GPa and 100 K. (b) Ionized ice VII at 305.7 GPa and 100 K. (c) Ice X at 605.7 GPa and 100 K. (d) Orientationally disordered ice VII at 5.7 GPa and 400 K. Black and open circles represent oxygens and hydrogens, respectively. O−H bonds are marked when the distance is less than 1.17 Å.

In the MD experiment II, a liquid water was cooled rapidly to yield a supercooled water. Then the pressure was increased from 8.4 to 608.4 GPa at a rate of 0.1 GPa per step. Furthermore, it was heated up to investigate high-pressure and high-temperature ice. We call this simulation III. In this calculation, the number of particles is chosen to be 810 (270 oxygens and 540 hydrogens), and the time step is taken to be $\Delta t = 0.4$ fs.

2. Results

2.1. MD Experiment I. *2.1.1. Simulation I.* Comparison of the pressure vs the volume of the system obtained by the present model with experimental data[7] (Figure 1) clearly shows that the predictions of pressure in the range of volume under consideration are too high compared with the experimental data. This implies nothing but a fault of the KKY potentials used in this work, the compressibility of the present model being too low. However, since the pressure is proportional to the derivative of the total energy with respect to the volume of the system, it should be rather sensitive to the forms of weak potentials of electrostatic origins, which are very difficult to know in general.

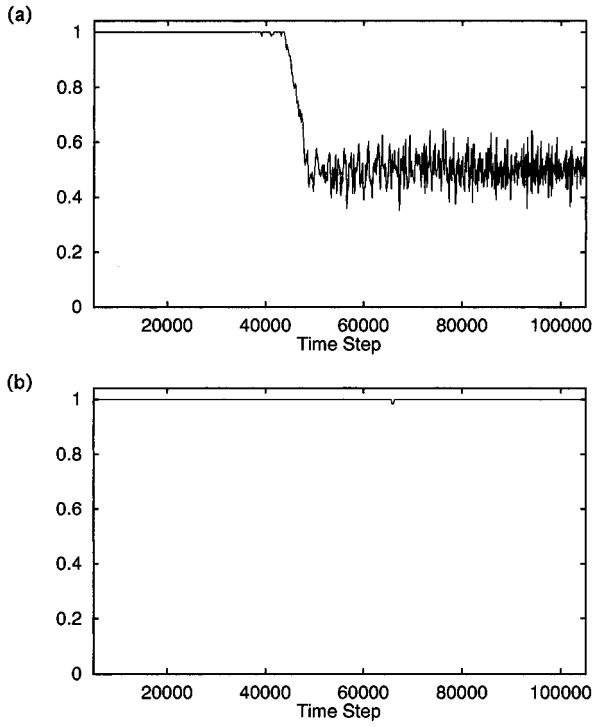

Figure 4. Probability of the two nearest-neighbor hydrogens around each oxygen at any time being the same as those at the initial time vs time steps for simulation I (a) and simulation II (b).

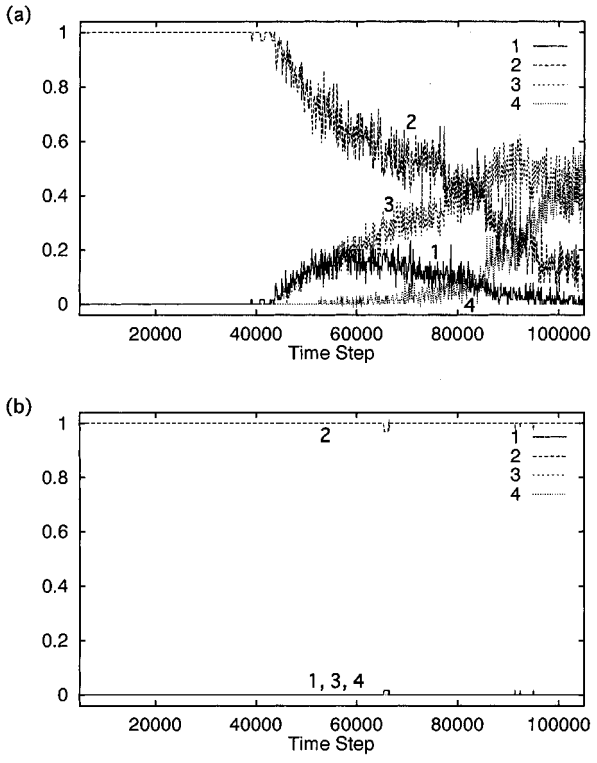

Figure 5. Probability that the average coordination number of hydrogens within a distance of 1.2 Å around each oxygen is 1, 2, 3, and 4 vs time steps for simulation I (a) and simulation II (b).

It is also shown that in both the present model and the experiments no clear anomalous behavior is observed in the volume−pressure curve, implying volume changes are not significantly accompanied by the phase transformations between ice VIII, ice VII, and ice X, if they happen as supposed by experiments or even a possibility that no phase change takes place up to this pressure range.

Figure 2 shows the partial pair distribution functions g_{OO}, g_{OH}, and g_{HH} obtained in simulation I. The dashed curves are

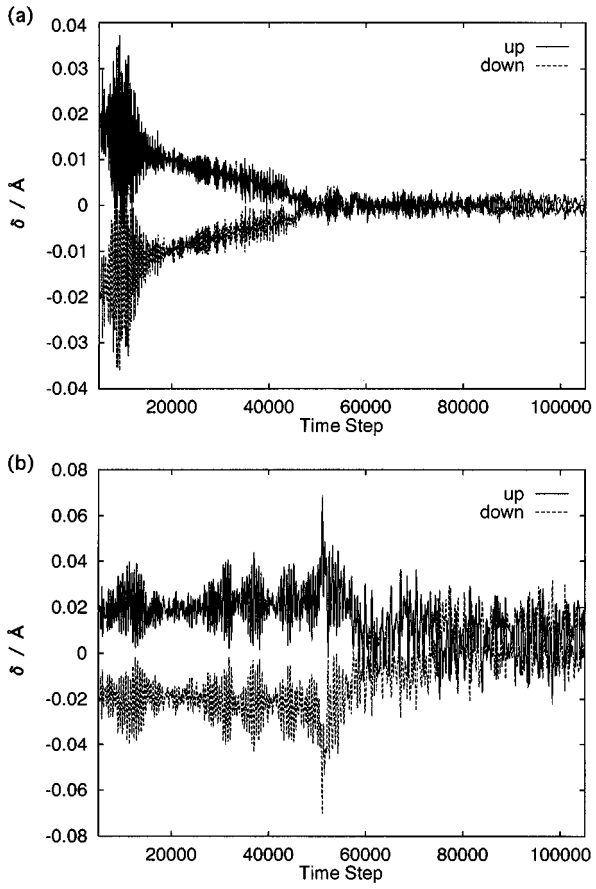

Figure 6. Variation of the distortion parameter δ vs time steps for simulation I (a) and simulation II (b). "up" and "down" correspond to the two oxygen sublattices initially displaced upward and downward, respectively.

the corresponding running coordination numbers. The top three figures are all for g_{OO}. The pressures are 5.7, 275.7, and 485.7 GPa from the top to the bottom, corresponding to ice VIII, VII, and X, respectively. The middle and the bottom three figures are for g_{OH} and g_{HH}, respectively, at the same pressures as the top figures. As the pressure is increased, the O−O distance and the O···H distance become shorter, while the O−H distance becomes longer, as seen in g_{OH}. In both ice VIII and ice VII, the running coordination number of g_{OH} at the first peak is 2, while in ice X, obviously 4 hydrogens are placed at the same distance from each oxygen, which is half the distance of the nearest O−O distance. The transition from ice VIII to ice VII takes place when the O−O distance becomes 2.43 Å, while the transition from ice VII to ice X takes place when the O−O distance becomes about 2.33 Å. Illustrations of ice VIII, VII, and X are shown in Figure 3.

The probability of the two nearest-neighbor hydrogens around each oxygen at any time being the same as those at the initial time is shown in Figure 4a. It is seen that hydrogen atoms are removed from original O−H bonds often, about 50 000 time steps.

We have calculated the probability that the average coordination number of hydrogens within a distance of 1.2 Å around each oxygen is 1, 2, 3, and 4 (Figure 5a). It turns out that as the VIII−VII transition takes place, the probability of the average coordination number being 1 and 3 becomes significant, and that of 2 remarkably decreases. This result indicates that a large number of ionic defects are caused by the VIII−VII transition.

We have monitored the distortion parameter δ of the oxygen lattice in ice VIII during simulation I (Figure 6a). The value of δ during the run of simulation I clearly indicates a change

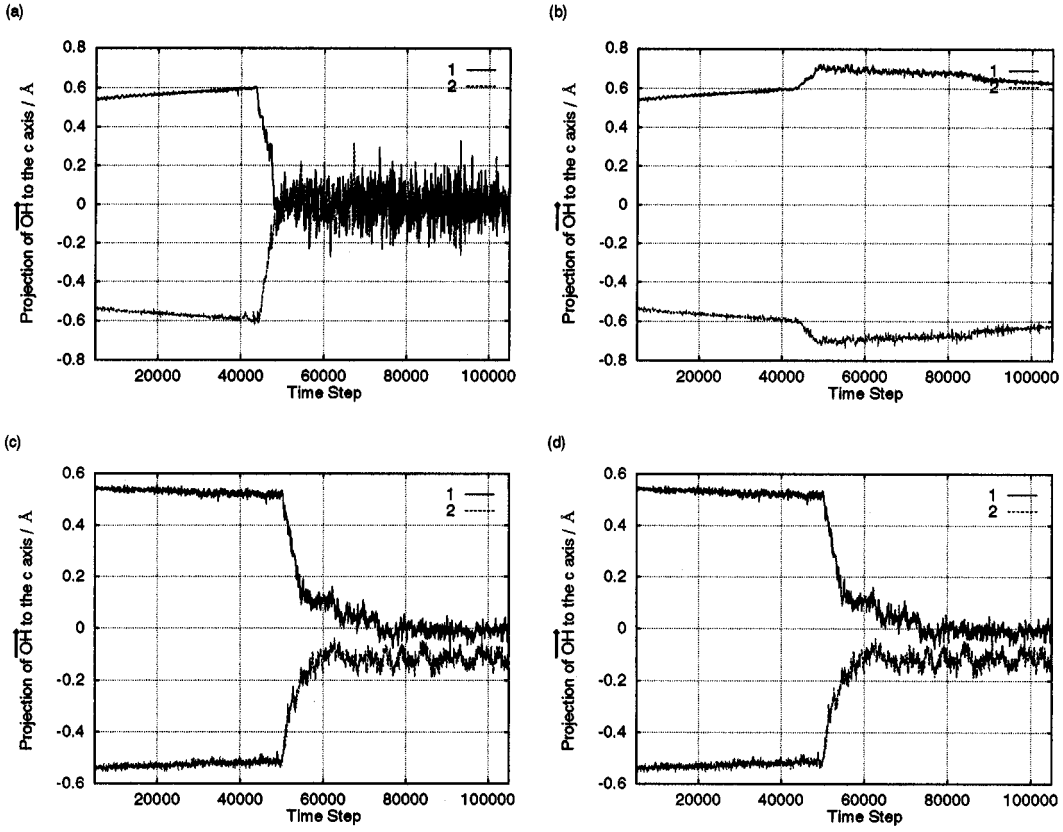

Figure 7. Averaged values of the projections of $\overrightarrow{OH}$'s to the *c* axis for the two sublattices in ice VIII. The solid line corresponds to the sublattice on which all the water molecules have upward dipole moments, while the dashed line corresponds to the sublattice on which all the water molecules have downward dipole moments. (a and b) Results for simulation I. (c and d) Results for simulation II. In parts a and c, $\overrightarrow{OH}$ is defined by the nearest or second nearest H around each O at time *t*. In parts b and d, $\overrightarrow{OH}$ is the same but with the O−H pair at $t = 0$.

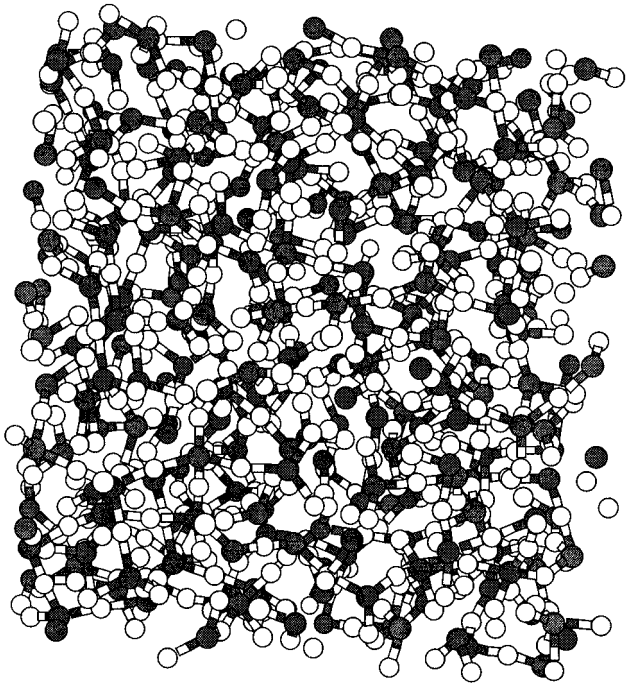

Figure 8. Hydrogen-bond-symmetrized amorphous ice. The same symbols as in Figure 3 are used.

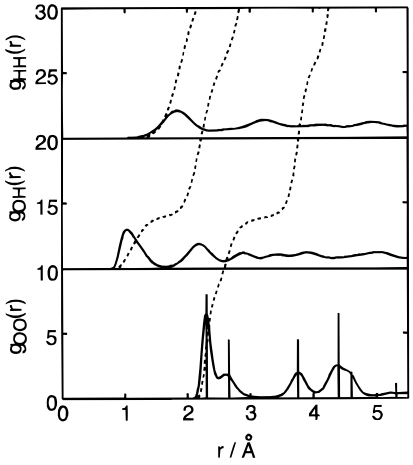

Figure 9. Partial pair distribution functions g_{OO}, g_{OH}, and g_{HH} (solid lines) and the corresponding running coordination numbers (dashed lines). The vertical lines in g_{OO} denote the ideal bcc peaks, the first peak of which is placed at the same position as that of g_{OO}.

of the crystalline structure from the sublattice structure of ice VIII to a single lattice with vanishing distortion δ.

The VIII−VII transition pressure predicted in this study is 275.7 GPa, which is much higher compared with the experimental value, which is less than 70 Gpa.[2,3] The hydrogen atom has to be treated as a quantum atom at low temperatures and/or high pressures. The main corrections are due to zero-point vibrations at low temperatures and tunneling effects at high pressures. In the present classical MD simulation we have neglected such quantum effects. The tunneling effect may cause the transition from ice VIII to ice VII and ice X and may lead to a lower value of pressure[19] than that predicted by the classical theory. However, as mentioned above, the pressure of the present model predicts too high a value. Therefore the pressure cannot be predicted accurately from the present model. This is rather a common tendency for any empirical model calculation which lacks the right information on weak attractions.

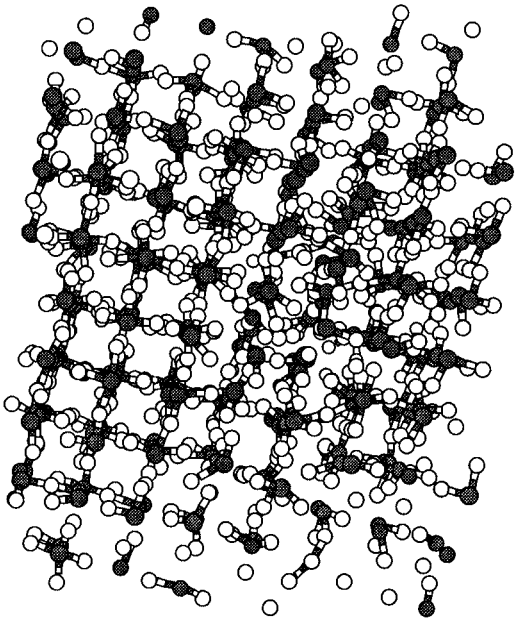

Figure 10. Ice X. The same symbols as in Figure 3 are used.

2.1.2. Simulation II. Orientationally disordered ice VII at low pressure and high temperature is shown in Figure 3d. From the analysis of the partial pair distribution functions g_{OO}, g_{OH}, and g_{HH}, it turned out that all these functions do not show any essential change during the run of the heating process; only some quantitative changes were observed, which show remarkable contrast to those obtained for simulation I. The first coordination number of hydrogens around each oxygen was always 2. The VIII−VII transition was observed in the annealing process at 400 K.

In Figure 4b, it is shown that the probability of the two nearest-neighbor hydrogens around each oxygen at any time being the same as those at the initial time is always 1 except for very rare cases. This means that no ionic defects are present and only the orientation of water molecules changes.

As shown in Figure 5b, the number of hydrogens within a distance of 1.2 Å around each oxygen is 2, indicating that the system consists of stable water molecules with no ionic defects, a remarkable contrast to the result for simulation I with increased pressure (Figure 5a).

The variation of the distortion value δ in simulation II is shown in Figure 6b. It vanishes when the VIII−VII transition takes place at about 60 000 time steps.

In order to know the orientational changes of the water molecules at the VIII−VII transition, we have calculated the averaged values of the projections of $\overrightarrow{OH}$'s to the *c* axis for each sublattice of ice VIII (Figure 7). Ice VIII consists of two different interpenetrating sublattices. On one sublattice all water molecules have upward dipole moments, and on the other sublattice all water molecules have downward dipole moments. We call the former sublattice 1 and the latter sublattice 2. The result for simulation I is shown in Figure 7a,b. The result for simulation II is shown in Figure 7c,d. In Figure 7a,c, $\overrightarrow{OH}$ is defined by the nearest or second nearest H around each O at time *t*. In Figure 7b,d, $\overrightarrow{OH}$ is defined in the same way but with the O−H pair at $t = 0$. The values are initially 0.54 and −0.54 Å for sublattice 1 and sublattice 2, respectively. In the case of simulation II, Figure 7c,d looks the same, since there is no exchange of O−H pairs as shown in Figure 4b. After the VIII−VII transition on heating, both the values for sublattice 1 and sublattice 2 are close to 0, indicating that orientational disordering of water molecules occurs at the transition. In the case of simulation I, as the pressure is increased, O−H length becomes longer, and after the VIII−VII transition, H's move between two potential minima (double-well potential). The results for simulation I are consistent with this. In Figure 7a, it turns out that the values are almost 0 after the transition because the two nearest H's around each O often change after the transition to ionic ice VII. In Figure 7b, the absolute values become rather larger after the transition to ionic ice VII takes place and gradually become smaller as the pressure is further increased.

These results of simulation II indicate that water molecules do not change their forms during the run upon heating, in marked contrast to the case of simulation I with increased pressure.

2.2. MD Experiment II. *2.2.1. Simulation III.* The amorphous ice obtained at 608.4 GPa and 400 K is shown in Figure 8, in which hydrogens are connected to the two nearest oxygens.[20] The partial pair distribution functions g_{OO}, g_{OH}, and g_{HH} and the corresponding running coordination numbers were calculated, and with these it turned out that the first peak of g_{OH} was located at about half the distance of that of g_{OO}, indicating hydrogen bond symmetrization. Experimentally, by compression of an amorphous ice, the transition to a crystalline phase close to ice VII is observed.[21] However, the conditions adopted in their work are not the same as our MD simulation. Applying pressure to an amorphous ice at an extremely high rate as in the present MD run to an extremely high pressure may transform it into a hydrogen-bond-symmetrized phase without crystallization.

We have raised the temperature of the amorphous ice from 400 K to 2400 K, after which a further MD run of 100 000 time steps was performed under constant-(*N*, *P*, *T*) ensemble. When the temperature was raised, the volume of the MD cell increased simultaneously, and after about 15 000 time steps, it decreased abruptly and at the same time the system was transformed into another state.

The partial pair distribution functions are shown in Figure 9. From g_{OO}, it is seen that the oxygen lattice is bcc. The position of the first peak of g_{OH} is half the distance of that of g_{OO}, indicating hydrogens are located at the midpoint of the two nearest oxygens. The running coordination number of the first peak of g_{OH} is 4. Thus, it can be concluded that ice X is obtained by heating the hydrogen-bond-symmetrized amorphous ice. This state was stable at least over more than 80 000 time steps after the transition. An illustration is shown in Figure 10.

The trajectories of oxygens and hydrogens during 20 000 time steps are shown in Figure 11. It is obvious that the hydrogens diffuse in the restricted area of a plane along which the oxygen lattice becomes disordered, indicating that defects play an important role in the proton diffusion in ice X. Such a tendency was continuously observed until the end of the present MD run at this pressure and temperature.

The temperature was raised from 2400 K to 16 000 K abruptly, after which a constant temperature−constant pressure MD simulation was continued for over 90 000 time steps. The length and angle of the MD cell changed rather often during the MD run, when oxygens repeated to form bcc and fcc from time to time. It follows that at this pressure and temperature the bcc lattice is not stable. Finally a state in which oxygens form an fcc lattice was obtained. The partial pair distribution functions are shown in Figure 12. From g_{OO} at 16 000 K, one cannot resolve the situation unambiguously, but quenching to a very low temperature, as shown in Figure 12, indicates that the oxygen lattice is not hcp but fcc. Ideally, in hcp, the g_{OO} should show 6 peaks and 56 neighbors up to around 5 Å, but in this figure there are 4 peaks with 12, 6, 24, and 12 neighbors,

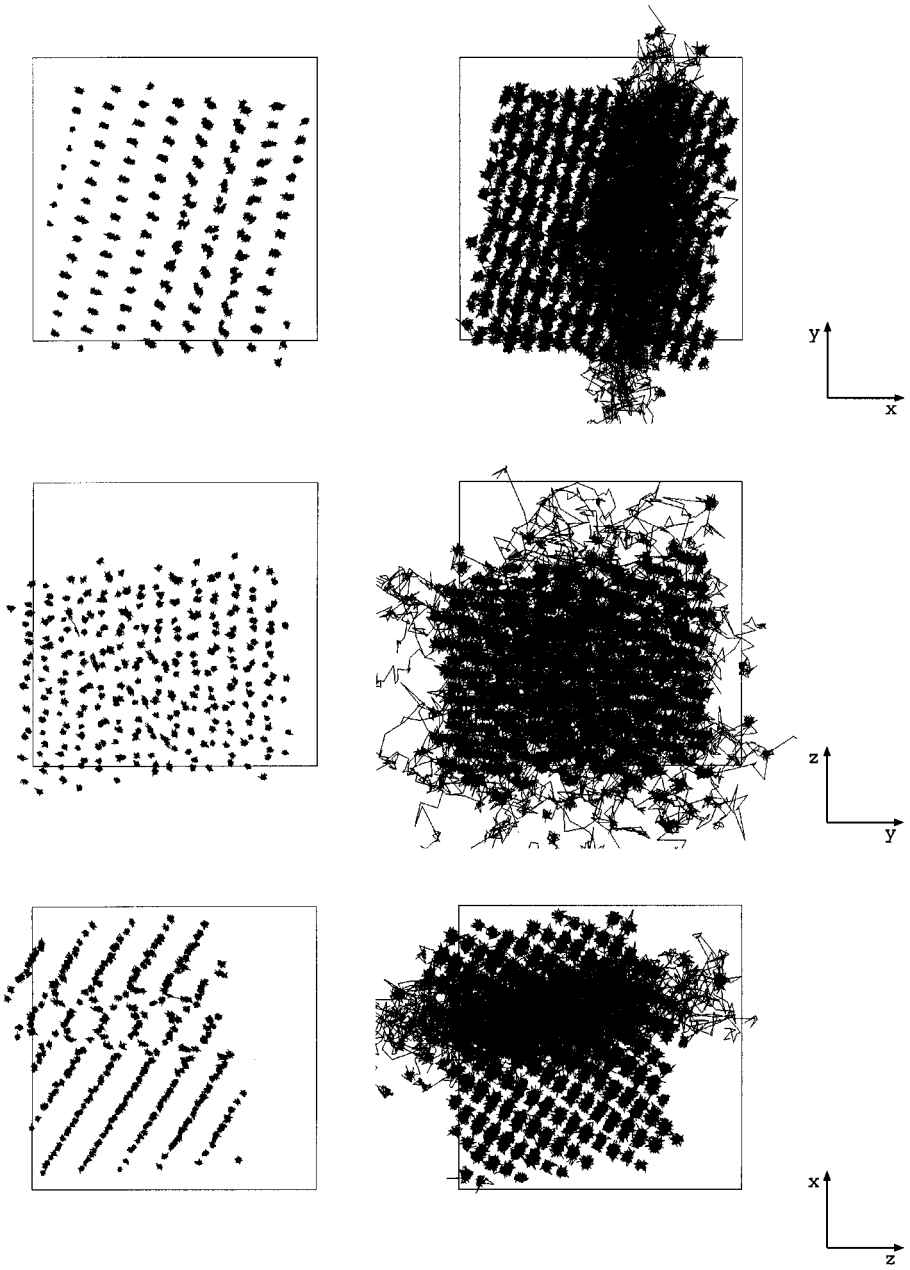

Figure 11. Trajectories of oxygens (left) and hydrogens (right) seen from the *z* direction (upper), *x* direction (middle), and *y* direction (lower), respectively. The uppermost figures correspond to Figure 10. The frames are to guide the eyes.

respectively, which is evidence of fcc structure. As seen from g_{HH}, protons are in an almost randomly distributed state with no correlations between them. The self-diffusion coefficient of protons was calculated from the slope of the mean-square displacement to yield 8.96×10^{-3} cm^2/s, which is more than 10^2 times larger than a typical liquid-like value due to the extremely high temperature of the system under consideration. An illustration is shown in Figure 13. The trajectories of oxygens and hydrogens are shown in Figure 14.

3. Conclusion and Discussion

Through simulation I, we have obtained the transition from ice VIII (proton-ordered state) to VII (proton-disordered state), which was transformed to ice X with a further increase in pressure. The transition from ice VIII with two different sublattices, which are distorted in the *c* direction, to ice VII with a single lattice at 275.7 GPa (6.64 cm^3/mol), was confirmed by monitoring the distortion parameter δ. On applying further pressure, it was confirmed that it was transformed into ice X at 485.7 GPa (5.89 cm^3/mol). Thus, the present result shows that ice VII intervenes between ice VIII and X in an appropriate range of high pressures, in agreement with the recent experiments by Pruzan *et al.*[2,3] The values of pressures at which the VIII−VII transformation and the VII−X transformation take place in simulation I may change somewhat if the pressure is increased more slowly and/or the simulation is done on a larger system. In the present classical MD simulation, we have neglected quantum effects. The values of pressures also change if the proton tunneling effect is taken into account. These considerations are beyond the present model.

The values of pressures obtained by the simulation are remarkably higher than the corresponding experimental values. This is nothing but to show that the present model is not sufficiently good to predict the pressure. Since the pressure is proportional to the derivative of the total energy with respect to the volume of the system, it is indeed difficult to reproduce the experimentally observed $P-V$ curve by means of any MD simulation in a wide range of pressure using as simple a potential model as constructed at a low-pressure ice. Moreover, the value of the pressure is not very sensitive to the structure of the system.

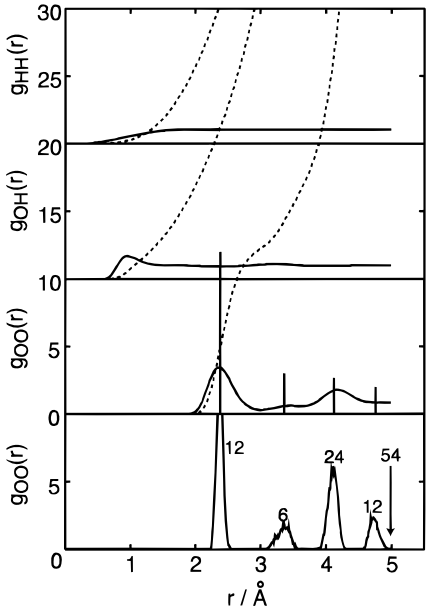

Figure 12. Partial pair distribution functions g_{OO}, g_{OH}, and g_{HH} (solid lines) and the corresponding running coordination numbers (dashed lines) (upper three figures). The vertical lines in g_{OO} denote the ideal fcc peaks with the first peak placed at the same position as that of g_{OO}. g_{OO} on quenching to a very low temperature (bottom figure) is also shown, in which peaks are shown with coordination numbers and the arrow at 5 Å indicates a total coordination of 54 oxygens.

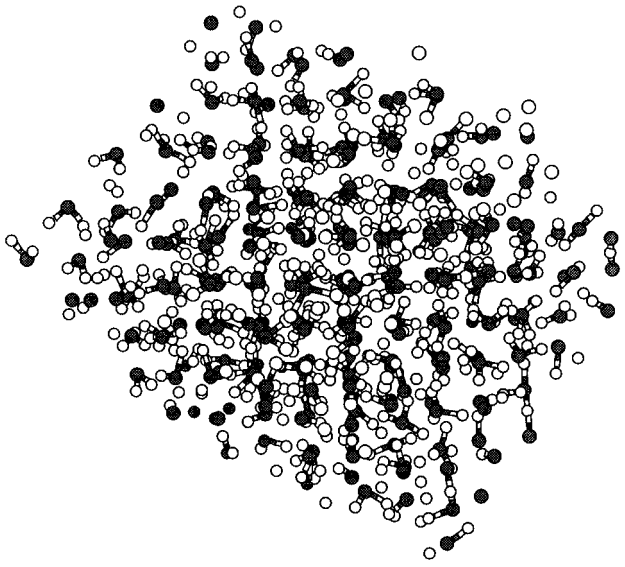

Figure 13. An fcc ice seen from the [100] direction of the fcc oxygen lattice. The same symbols as in Figure 3 are used.

The volumes at which transitions occur (the prediction for the VIII−VII transition being 6.6 cm^3/mol and that for the VII−X transition being 5.9 cm^3/mol) are in agreement with experiments (VII−X transition takes place at about 6 cm^3/mol). Many of the results that have been obtained through the present model for water and ice are well compatible with the experiments.

Through simulation II, we have obtained the transition from ice VIII to ice VII. It has been made clear that the transitions observed under the processes of both simulations I and II result from entirely different mechanisms. During the structural transformation from ice VIII to X on applying pressure (simulation I), ice VII appears. The structure of ice VII thus obtained differs from that of ice VII obtained by heating of ice VIII at a normal pressure (simulation II). The latter is accompanied by orientational disorder, while the former contains ionic defects.

Through simulation III, we have performed isothermal MD simulation by applying pressure, and after that we have performed an isobaric heating MD simulation. By a rapid compression of a supercooled water, a hydrogen-bond-symmetrized amorphous ice was obtained, although it has experimentally been suggested that an amorphous ice crystallizes by applying pressure. The result may depend on the process of the experiments.

By heating, it crystallized into ice X. Amorphous ices can be crystallized by increasing temperature, as commonly observed in experiments.[21,22] However, this is not trivial in MD simulations, because crystallization in a rather small system (liquid) is generally difficult to observe. The present result of the MD simulation is specific from this point of view, since it shows a partial crystallization from an amorphous ice. In ice X obtained, the bcc oxygen lattice was not completely ordered but involved disordered layers. Hydrogens diffuse in such disordered layers, indicating that defects of the oxygen lattice play an important role in proton diffusion in crystalline ice X.

The problem of what is the next phase to ice X is a very interesting subject in the high-pressure ice study.[23,24] By raising the temperature of high-pressure ice X, a possibility of a new phase has been proposed. The present MD simulation suggests that at a temperature about as high as ice X melts and at a pressure where the ice X is stable, a phase appears in which the oxygen lattice forms fcc and hydrogens are diffusive, similar to the superionic conductor reported by Demontis *et al.*[23]

References and Notes

(1) Fletcher, N. H. *The Chemical Physics of Ice*; Cambridge University Press: New York, 1970; Chapter 3.

(2) Pruzan, Ph.; Chervin, J. C.; Canny, B. *J. Chem. Phys.* **1992**, *97*, 718.

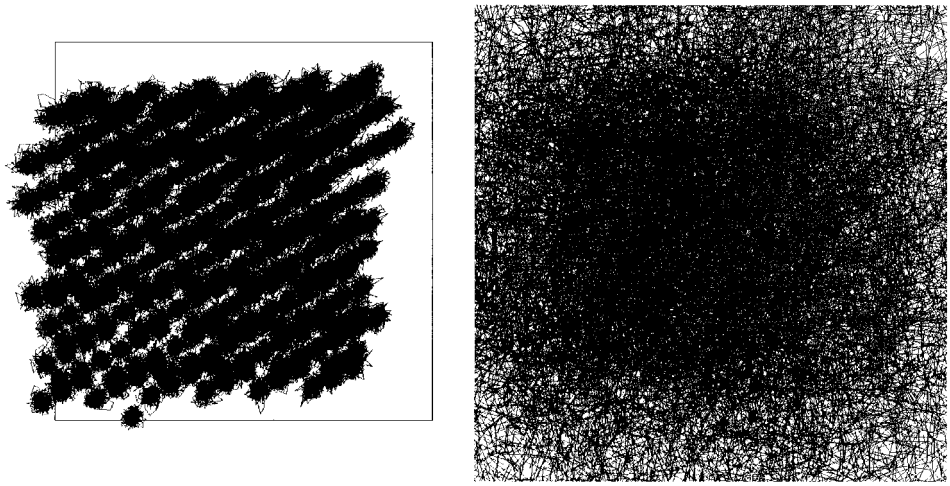

Figure 14. Trajectories of oxygens during 10 000 steps (left) and hydrogens during 200 steps (right). The frames are to guide the eyes.

(3) Pruzan, Ph.; Chervin, J. C.; Canny, B. *J. Chem. Phys.* **1993**, *99*, 9842.
(4) Hirsch, K. R.; Holzapfel, W. B. *Phys. Lett. A* **1984**, *101*, 142.
(5) Hirsch, K. R.; Holzapfel, W. B. *J. Chem. Phys.* **1986**, *84*, 2771.
(6) Polian, A.; Grimsditch, M. *Phys. Rev. Lett.* **1984**, *52*, 1312.
(7) Hemley, R. J.; Jephcoat, A. P.; Mao, H. K.; Zha, C. S.; Finger L. W.; Cox, D. E. *Nature* **1987**, *330*, 737.
(8) Schweizer, K. S.; Stillinger, F. H. *J. Chem. Phys.* **1984**, *80*, 1230.
(9) Holzapfel, W. B. *J. Chem. Phys.* **1972**, *56*, 712.
(10) Goncharov, A. F.; Struzhkin, V. V.; Somayazulu, M. S.; Hemley, R. J.; Mao, H. K. *Science* **1996**, *273*, 218.
(11) Kumagai, N.; Kawamura, K.; Yokokawa, T. *Mol. Simul.* **1994**, *12*, 177.
(12) Matsuoka, O.; Clemeni, E.; Yoshimine, M. *J. Chem. Phys.* **1976**, *64*, 1351.
(13) Impey, R. W.; Klein M. L.; Tse, J. S. *J. Chem. Phys.* **1984**, *81*, 6406.
(14) Hashimoto, T.; Sugawara, S.; Hiwatari, Y. *Mol. Simul.* **1996**, *18*, 115.
(15) Parrinello, M.; Rahman, A. *Phys. Rev. Lett.* **1980**, *45*, 1196.
(16) Parrinello, M.; Rahman, A. *J. Appl. Phys.* **1981**, *52*, 7182.
(17) Kuhs, W. F.; Finney, J. L.; Vettier, C.; Bliss, D. V. *J. Chem. Phys.* **1984**, *81*, 3612.
(18) Nosé, S. *J. Chem. Phys.* **1984**, *81*, 511.
(19) Lee, C.; Vanderbilt, D.; Laasonen, K.; Car, R.; Parrinello, M. *Phys. Rev. B* **1993**, *47*, 4863.
(20) Hashimoto, T.; Oda, T.; Hiwatari, Y. *Mol. Simul.* **1997**, *18*, 395.
(21) Hemley, R. J.; Chen, L. C.; Mao, H. K. *Nature* **1989**, *338*, 638.
(22) Mishima, O. *J. Chem. Phys.* **1994**, *100*, 5910.
(23) Demontis, P.; LeSar, R.; Klein, M. L. *Phys. Rev. Lett.* **1988**, *60*, 2284.
(24) Benoit, M.; Bernasconi, M.; Focher, P.; Parrinello, M. *Phys. Rev. Lett.* **1996**, *76*, 2934.